

Production of QED pairs at small impact parameter in relativistic heavy ion collisions

Kai Hencken, Gerhard Baur, Dirk Trautmann

October 23, 2018

Abstract

The STAR collaboration at RHIC is measuring the production of electron-positron pairs at small impact parameters, larger than but already close to the range, where the ions interact strongly with each other. We calculate the total cross section, as well as, differential distributions of the pair production process with the electromagnetic excitation of both ions in a semiclassical approach and within a lowest order QED calculation. We compare the distribution of electron and positron with the one coming from the cross section calculation without restriction on impact parameter. Finally we give an outlook of possible results at the LHC.

1 Introduction

Pair production in relativistic heavy ion collisions has attracted interest in the past mainly due to the fact that the strong fields allow for multiple pairs to be produced. At impact parameter of the order of twice the nuclear radius, but still larger than this, so that the two ions do not interact hadronically with each other (that is the regime of the so-called “ultraperipheral collisions” UPC), the total pair production multiplicity is found to be about 1.5 for AuAu collisions at RHIC and about 3.9 for PbPb collisions at the LHC. These results are based on a lowest order QED calculation [1] and one might suspect that at these small impact parameters the strong fields of the two ions do lead to higher order corrections.

Therefore it is of interest to measure electron-positron pairs produced in such collisions and compare their distribution with theoretical predictions, e.g., in lowest order QED. The STAR collaboration has recently measured e^+e^- pairs in collisions, which were selected by a trigger, looking for the simultaneous excitation of the two ions (mainly to the GDR) in addition to the pair production process [2, 3, 4], see Fig. 1. Such an event is characterized by the subsequent emission of one or only a few neutrons, which are then detected in the forward ZDC (“Zero Degree Calorimeter”). This tagging was first proposed in order to study vector meson production [5, 6, 7]. Mutual excitation of the two ions is also used for the luminosity measurement at RHIC [8, 9].

As the average impact parameter in such collisions is only about [10]

$$\bar{b} = \frac{\int d^2b bP(b)}{\int d^2bP(b)} \approx \frac{8R_a}{3} \approx 19 \text{ fm}, \quad (1)$$

one may expect strong field effects to be present for the pairs.

Due to the design of the STAR detector only electrons and positrons having a transverse momentum $p_t > 65$ MeV/c and being emitted with a rapidity $|y| < 1.15$ can be detected. As most of the pairs produced in ultraperipheral collisions (UPCs) are emitted with energies of the order of a few $m_e c^2$ and at small angles, such a measurement can only look at the tails of the distribution of the pairs. Even this momentum range was only possible due to a lowered magnetic field in the STAR detector.

One approach to the calculation of this process is the use of the impact parameter dependent equivalent photon approximation [11, 12, 13, 14]. The additional electromagnetic processes are easily incorporated in this semiclassical approach and the cross section can be expressed as

$$\frac{d^6\sigma_{e^+e^-,2GDR}}{d^3p_+d^3p_-} = \int d^2b P_{GDR}^2(b) \frac{d^4L}{d^2bd\omega_1d\omega_2} \frac{d^6\sigma_{\gamma\gamma\rightarrow e^+,e^-}(\omega_1, \omega_2)}{d^3p_+d^3p_-}. \quad (2)$$

where $\sigma_{\gamma\gamma\rightarrow e^+,e^-}$ denotes the cross section for real photons and $d^4L/d^2bd\omega_1d\omega_2$ the impact parameter dependent photon-photon luminosity (for the details of the photon-photon luminosity, see Sec. 2.7 of [15] and references therein). One difficulty in this approach is the correct choice of the cutoff parameter present in the expression for the photon spectrum. This is especially difficult due to the smallness of m_e , which is much smaller than the “usual cutoff” imposed on the maximal transverse momentum of the photon from the elastic form factor of the ion, which is given by $1/R_A \approx 80$ MeV. It was found that the total cross section for electron-positron pair production is only reproduced with a cutoff chosen around m_e . On the other hand it was also found that neither a choice of m_e nor of R_A is able to predict the total probability at impact parameter smaller than the Compton wave length $\lambda_c = 386$ fm [1]. For a discussion about the choice of the impact parameter see, e.g., [16]. In addition in the usual semiclassical approach the transverse momentum distribution of the photons is integrated over. In order to get, for example, the transverse momentum distribution of the pair, one needs to take this momentum distribution into account to get the correct final result. For a possible approach taking this into account from first principles see [17, 18].

In Section 2 we show how our calculation is done in lowest order QED and in the semiclassical approximation. This is then used in Sec. 3 to calculate total cross sections, differential distributions for RHIC and also for possible LHC conditions. The comparison with the experimental results has been done in the meantime and will be presented by the STAR collaboration in another publication [19].

2 Calculation of pair production and nuclear excitation in lowest order QED

The STAR experiment at RHIC measures the pair production cross section together with the double electromagnetic excitation in both ions, see Fig. 1. In order to incorporate the experimental conditions in the theoretical calculation, it is most appropriate to work in the semiclassical approach. Using the fact, that in this approach the probabilities of the individual processes factorize and are given by the product of the individual probabilities

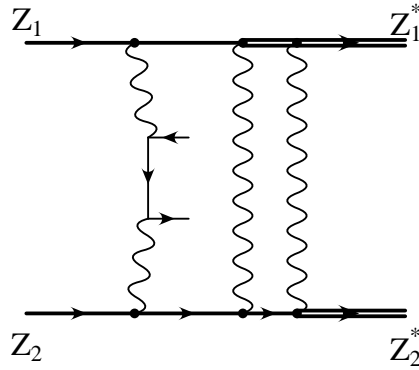


Figure 1: The pair production together with the electromagnetic excitation of both ions, predominantly to the giant dipole resonance (GDR) is shown as one typical Feynman diagram. The process in lowest order involves at least the exchange of four photons (many more “soft Coulomb photons” are exchanged as well). Due to this the process predominantly occurs at small impact parameter, where the electromagnetic fields are strong, in contrast to the unrestricted cross section (without electromagnetic excitation of the ions), which has contributions coming also from large impact parameters.

(for a theoretical description of this approach, see [10]) we can write the cross section for this process as

$$\frac{d^6\sigma_{e^+e^-,2GDR}}{d^3p_+d^3p_-} = 2\pi \int_{b_{min}}^{\infty} bdb P_{GDR}^2(b) \frac{d^6P(b)}{d^3p_+d^3p_-}. \quad (3)$$

The minimum impact parameter was chosen to be $b_{min} = 2R_a \approx 14\text{fm}$, where we assume the nuclei to touch, that is, interact hadronically with each other. The use of the semiclassical description in this case is not only justified due to the strong Coulomb interaction between the two ions (leading to a large number of “soft” Coulomb photons exchanged between them), but also simplifies the calculation of this higher order process (pair production plus two GDR excitation processes) considerably.

Following [20] the probability for GDR excitation in one ion is to a good approximation given as

$$P_{GDR}(b) = S/b^2 \quad (4)$$

with

$$S = \frac{2\alpha^2 Z^3 N}{Am_N \omega} \approx 5.45 \times 10^{-5} Z^3 N A^{-2/3} \text{fm}^2. \quad (5)$$

where m_N denotes the nucleon mass, and the neutron-, proton-, and mass-number of the ions are N, Z , and A respectively (we consider only symmetric collisions here, the calculation can trivially be extended to incorporate also asymmetric systems). The excitation probability is inversely proportional to the energy ω ($\approx 80\text{MeV}A^{-1/3}$) of the GDR state. Neutrons are not only emitted from the GDR excitation but are also coming from higher excited states [8, 21, 22]. These can be taken into account approximately by increasing S accordingly. As this does not change the $1/b^2$ behavior for the small impact parameter, we are interested in, and only leads to a rescaling of the total cross section, not the form of the differential distributions, we have used in our calculation the more simple value of S in Eq. (5). Of course one needs then to include in addition the different decay channels into one, two, etc. neutrons [23, 24, 25], as well as, the fact that the probability for

GDR excitation is already quite large (about 0.5 for b_{min}) so that multiphoton excitation mechanisms need to be included as well. Assuming a Poisson distribution for the different (independent) excitation processes, one would need to replace $P_{GDR}(b)$ then with [21]

$$P(b) = 1 - \exp(P_{GDR}(b)). \quad (6)$$

One sees that the multiphoton excitation tends to reduce again the probability (it has to stay below the unitarity limit of 1). In the appendix we show how a more complex b dependence than a simple $1/b^2$ for $P_{GDR}(b)$ can be calculated within the same approach. Therefore an improved calculation can be done in this way. On the other hand for the current experimental accuracy the simplified approach seems to be appropriate.

With this the cross section for pair production together with the GDR excitation of both ions is given by

$$\frac{d^6\sigma_{e^+e^-,2GDR}}{d^3p_+d^3p_-} = 2\pi \int_{b_{min}}^{\infty} bdb P_{GDR}^2(b) 2\pi \int qdq \frac{d^6\hat{P}(q)}{d^3p_+d^3p_-} J_0(qb) \quad (7)$$

$$= (2\pi)^2 S^2 \int qdq \frac{d^6\hat{P}(q)}{d^3p_+d^3p_-} \int_{b_{min}}^{\infty} bdb \frac{J_0(qb)}{b^4} \quad (8)$$

$$= (2\pi)^2 S^2 \int qdq \frac{d^6\hat{P}(q)}{d^3p_+d^3p_-} \int_{b_{min}}^{\infty} \frac{db}{b^3} J_0(qb) \quad (9)$$

where we have introduced the two-dimensional Fourier transform of the impact parameter dependent probability for pair production $d^6P(b)/d^3p_+d^3p_-$ as

$$\frac{d^6P(b)}{d^3p_+d^3p_-} = \int d^2q \exp(i\vec{q}\vec{b}) \frac{d^6\hat{P}(\vec{q})}{d^3p_+d^3p_-} = 2\pi \int qdq \frac{d^6\hat{P}(q)}{d^3p_+d^3p_-} J_0(qb) \quad (10)$$

We rewrite the integral over b in dimensionless units as

$$\int_{b_{min}}^{\infty} \frac{db}{b^3} J_0(qb) = q^2 \int_{qb_{min}}^{\infty} \frac{dx}{x^3} J_0(x) =: q^2 I_3(qb_{min}). \quad (11)$$

Following the derivation of [1, 26], one can calculate the two-dimensional Fourier transform $\frac{d^6P(\vec{b})}{d^3p_+d^3p_-}$ in lowest order QED. The two Feynman diagrams for this process in the semiclassical approximation are shown in Fig. 2. One gets the differential probability as

$$\begin{aligned} \frac{d^6\hat{P}(q)}{d^3p_+d^3p_-} &= (Z\alpha)^4 \frac{4}{\beta^2\gamma^4} \frac{1}{(2\pi)^6 2\epsilon_+ 2\epsilon_-} \int d^2q_1 [N_0 N_1 N_3 N_4]^{-1} \\ &\times \text{Tr} \left\{ (\not{p}_- + m) \left[N_{2D}^{-1} \not{\psi}^{(1)} (\not{p}_- - \not{q}_1 + m) \not{\psi}^{(2)} + N_{2X}^{-1} \not{\psi}^{(2)} (\not{q}_1 - \not{p}_+ + m) \not{\psi}^{(1)} \right] \right. \\ &\left. \times (\not{p}_+ - m) \left[N_{5D}^{-1} \not{\psi}^{(2)} (\not{p}_- - \not{q}_1' + m) \not{\psi}^{(1)} + N_{5X}^{-1} \not{\psi}^{(1)} (\not{q}_1' - \not{p}_+ + m) \not{\psi}^{(2)} \right] \right\}. \end{aligned} \quad (12)$$

with

$$\begin{aligned} N_0 &= -q_1^2, & N_1 &= -(q_1^2 - (p_+ + p_-))^2, \\ N_3 &= -(q_1 + q)^2, & N_4 &= -[q_1 + (q - p_+ - p_-)]^2, \end{aligned}$$

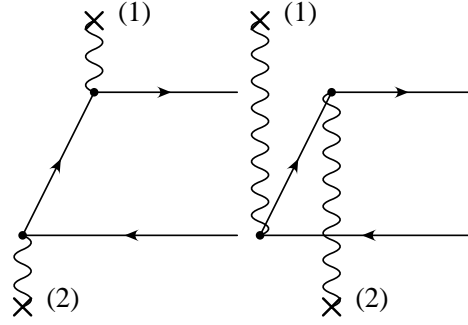


Figure 2: The two Feynman diagrams contributing to pair production in lowest order QED are shown. The crossed denote the coupling to the (external) Coulomb field of one of the ions.

$$N_{2D} = -(q_1 - p_-)^2 + m^2, N_{2X} = -(q_1 - p_+)^2 + m^2,$$

$$N_{5D} = -[q_1 + (q - p_-)]^2 + m^2, N_{5X} = -[q_1 + (q - p_+)]^2 + m^2,$$

with the longitudinal component of q_1 given by $q_{10} = \frac{1}{2}[(\epsilon_+ + \epsilon_-) + \beta(p_{+z} + p_{-z})]$, $q_{1z} = \frac{1}{2\beta}[(\epsilon_+ + \epsilon_-) + \beta(p_{+z} + p_{-z})] = \frac{1}{\beta}q_{10}$ and $u^{(1,2)} = \gamma(1, 0, 0, \pm\beta)$ are the four velocity of the two ions, γ and β the Lorentzfactor and velocity of each ion in the center of mass frame. We have included in addition a nuclear form factor $F(q)$. We choose for ease of computation in our case a monopole form factor of the form

$$F(q) = \frac{\Lambda^2}{\Lambda^2 - q^2} = \frac{\Lambda^2}{\Lambda^2 + Q^2} \quad (13)$$

where $\Lambda^2 = \frac{6}{\langle R^2 \rangle}$ is set to about 80 MeV in order to reproduce the rms radius of the ion. This leads in the terms N_0^{-1} , N_1^{-1} , N_3^{-1} and N_4^{-1} to a replacement of the term $1/q^2$ by $F(q)/q^2$. The integration over d^2q_1 can be done analytically, using the usual tricks for Feynman integrations in two dimensions. For details of this, we refer the reader to [1].

The integral $I_3(z = qb_{min})$ in Eq. (11) can be solved analytically and calculated easily, as is shown in the appendix.

Finally we make the integral over dq dimensionless to get

$$\frac{d^6\sigma_{e^+e^-, 2GDR}}{d^3p_+d^3p_-} = (2\pi)^2 \frac{S^2}{b_{min}^4} \int z^3 dz \frac{d^6\hat{P}\left(\frac{z}{b_{min}}\right)}{d^3p_+d^3p_-} I(z). \quad (14)$$

For the unrestricted differential cross section (that is without triggering on the additional electromagnetic excitations of the ions), we integrate over \vec{b} without the factor $P_{GDR}^2(b)$ in Eq. (3). As the contribution coming from $b < b_{min}$ is small, we have extended the integration over all b .

$$\begin{aligned} \frac{d^6\sigma_{e^+e^-}}{d^3p_+d^3p_-} &= \int d^2b \frac{d^6P(b)}{d^3p_+d^3p_-} \\ &= \int d^2b d^2q \frac{d^6\tilde{P}(q)}{d^3p_+d^3p_-} \exp(i\vec{q}\vec{b}) \\ &= (2\pi)^2 \int d^2q \delta(\vec{q}) \frac{d^6\hat{P}(q)}{d^3p_+d^3p_-} \end{aligned}$$

$$= (2\pi)^2 \frac{d^6 \hat{P}(0)}{d^3 p_+ d^3 p_-}. \quad (15)$$

This approach was pursued in [26] and total and differential cross sections were calculated. For the unrestricted cross sections we do not take a nuclear form factor of the two ions into account, as pair production occurs predominantly at large impact parameter and for small q^2 of the two photons.

Whereas for the unrestricted cross section only the value of $\hat{P}(q)$ for $q = 0$ is needed, here our expression is a folding over a range of q given in terms of $1/b_{min}$. In order to compare the differential distributions in both the restricted and in the unrestricted case we have also made calculations of the unrestricted cross section with the same kinematical restrictions as in the case with GDR excitations.

The expression of Eq. (14) is in a form, which can be evaluated using a Monte Carlo integration for both the integration over z , as well as, the six-dimensional integration over p_+ and p_- at the same time. For this we have used VEGAS [27]. Both $P(q)$ and J_0^{int} are oscillatory functions, having both positive and negative values, which could lead to cancellations. Looking at $z^3 I(z)$ together with the result of $P(z/b_{min})$ one sees that the integrand falls off for large z , that is for large q . It is found that the main contribution comes from the region around $z = 2$ and that the contribution from the negative part at larger z are suppressed. The integration will have positive and negative contributions but the cancellations between them are not severe. With the help of VEGAS we can get the total cross section and also differential cross sections by binning the differential results.

3 Results

We have made calculations of the total cross section and differential distributions of the electron, the positron and the pair including the experimental restrictions at STAR. The integration over b (or equivalently q) is incorporated into the Monte Carlo integration. Another strategy would be to calculate $d^6 \hat{P}(q)/d^3 p_+ d^3 p_-$ for different values of q and fixed values of p_+ , p_- and do a Bessel transform in each case. For the total cross section, that is $\hat{P}(q)$, this can be done and was done as an independent check of our approach. To obtain differential cross sections, this approach is rather cumbersome.

In a first step, we have calculated the total cross section as a function of b_{min} , the minimum impact parameter, by using three different approaches: We can calculate $P(b)$ directly for the pair production process and integrate numerically over b . Second we can start from $\hat{P}(q)$ directly and do the integration over q numerically via the Fourier transformed of $P_{GDR}(b)$, that is, using $I(z)$. Finally we have done the calculation with the integration over q , that is z , directly with the Monte Carlo integration. In all three cases we have restricted the phase-space integration over the momenta of electron and positron according to the experimental conditions of STAR: $p_t > 60$ MeV/c and $|y| < 1.15$ for each lepton. The results are shown in Fig 3. The lines correspond to calculations with and without a monopole form factor for the nucleus, showing that the incorporation of a form factor is important. All three results agree quite well with each other, showing that our approach is working well.

From this we get a total cross section for AuAu collisions at RHIC, including the restrictions $|p_t| > 60$ MeV/c, $|y| < 1.15$ of 2.30, 1.76, 1.43 mb, for $b_{min} = 13, 14$ and

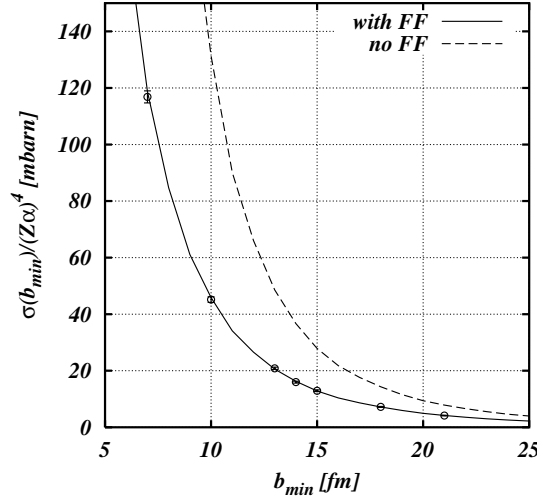


Figure 3: The total cross section including kinematical restrictions of the STAR experiment are shown as a function of the minimal allowed impact parameter b_{min} . Calculations with and without a form factor for the nucleus are shown. The lines were calculated by calculating $P(b)$ first and integrating then over b . These lines are in perfect agreement with a similar approach, where $P(q)$ is calculated first and then integrated over q . The circles correspond to the results of our Monte Carlo approach, where, as explained in the text, both the integration over q and over p_+ and p_- are done within the Monte Carlo integration routine.

15 fm, respectively. In addition we have calculated a number of differential distributions, which were also studied at STAR. The transverse momenta and energy distribution of the electron and positron are shown in Fig. 4. In lowest order QED the distribution of electron and positron are identical to each other. The difference between the two distributions can therefore be seen as a measure of the accuracy the MC integration. One can look also at properties of the produced pair: The transverse momentum and the invariant mass of the pair are shown in Fig. 5. We have not shown the rapidity distribution, which we found to be more or less flat over the allowed range. In all four diagrams we show also the differential distributions of the unrestricted cross section. We have rescaled the data, so that the total cross section are the same in both cases. We see that the transverse momentum distribution and the energy distribution of the individual leptons are more or less identical in shape. The same is also true for the invariant mass distribution, with the only exception that the “tail” at low invariant masses is higher for the unrestricted distributions. The biggest effect is seen in the transverse momentum distribution of the pair. Here we also expect the effect of the small impact parameter (corresponding to larger transverse momenta of the photons) to be largest. The slower fall-off at larger transverse momenta is most probably due to the fact that no form factor was used in the calculation of this cross section, which should be visible at $P_t > 80$ MeV/c. In order to investigate the effect of the nuclear form factor and in order to understand the large difference between the cross section with and without nuclear form factor, see Fig. 3 above, we show in this plot also the transverse momentum distribution of the pair for a calculation without form factor. It can be seen that in this case the cross section gets sizeable contributions for $P_t > 80$ MeV/c.

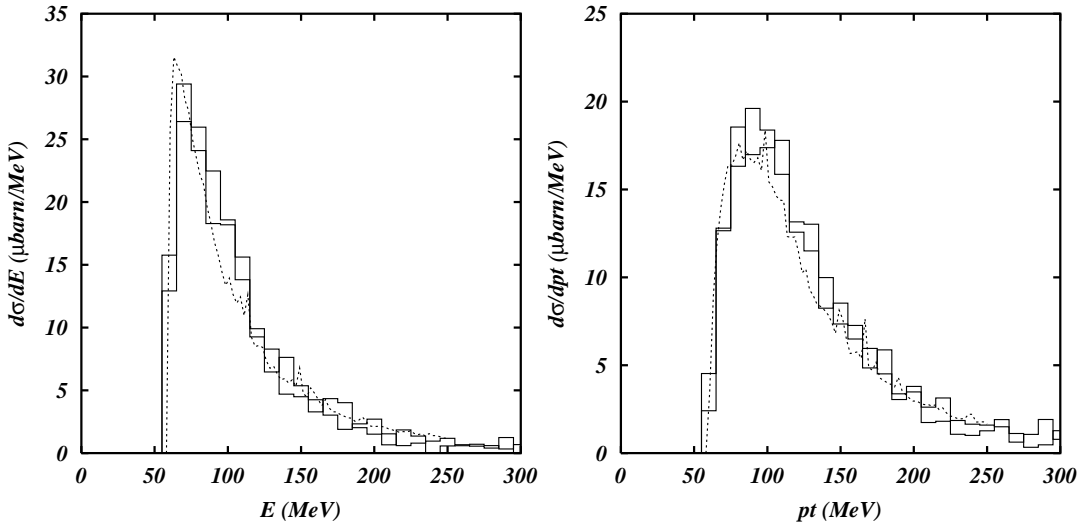


Figure 4: Energy and transverse momentum distribution are shown for the electron and the positron. In lowest order QED the two distributions are identical and the spread between the two is a measure of the uncertainties coming from the Monte Carlo integration. This is compared with a unrestricted cross section calculation (dotted line), normalized to give the same total cross section.

We have studied in addition the question, whether especially the distribution as a function of P_t of the pair is sensitive to the form of $P_{GDR}(b)$ used in our approach. Using a more general approach, see appendix for details, one expects that the next correction is of the form $P_{GDR}^3(b) \sim 1/b^6$ instead of $P_{GDR}^2(b) \sim 1/b^4$. In such a model the average impact parameter changes from about $\frac{8R_a}{3} \approx 19$ fm to about $\frac{12R_a}{5} \approx 17$ fm, which is a small change compared to the Compton wavelength of the electron (400 fm), but is still a 10% reduction of this average impact parameter. We have therefore studied the distribution of electron and positron for this restriction. As expected the differential distributions are found to be the same within the uncertainties of the Monte Carlo approach used.

As an outlook for future experiments we are showing results and distributions one might expect to see for PbPb collisions at the LHC. Using the same kinematical restrictions as for the STAR experiment, the results are shown in Fig. 6 and 7.

As a rather optimistic estimate we have calculated also the differential cross section for a kinematical range of $|p_t| > 2.6$ MeV/c and $|y| < 1.5$, where ALICE will be able to detect the electrons with its Internal Trigger System (ITS), even though it will not be able to measure energies or momenta.

With these kinematical conditions we can study the question, whether ALICE will be able to see multiple pairs produced in a single collisions. For this we calculate the impact parameter dependent cross section under the kinematical conditions. One finds that for impact parameters close to b_{min} $P(b) \approx 20\%$. Following [28, 26, 29, 30] we use a Poisson distribution as a good approximation for the N pair production probability

$$P(N, b) = \frac{P(b)^N}{N!} \exp(-P(b)) \quad (16)$$

Multiplying with $P_{GDR}^2(b)$ and integrating over b we get the cross section for one, two, ... pair production. The result as a function of b_{min} is shown in Fig. 8 together with the

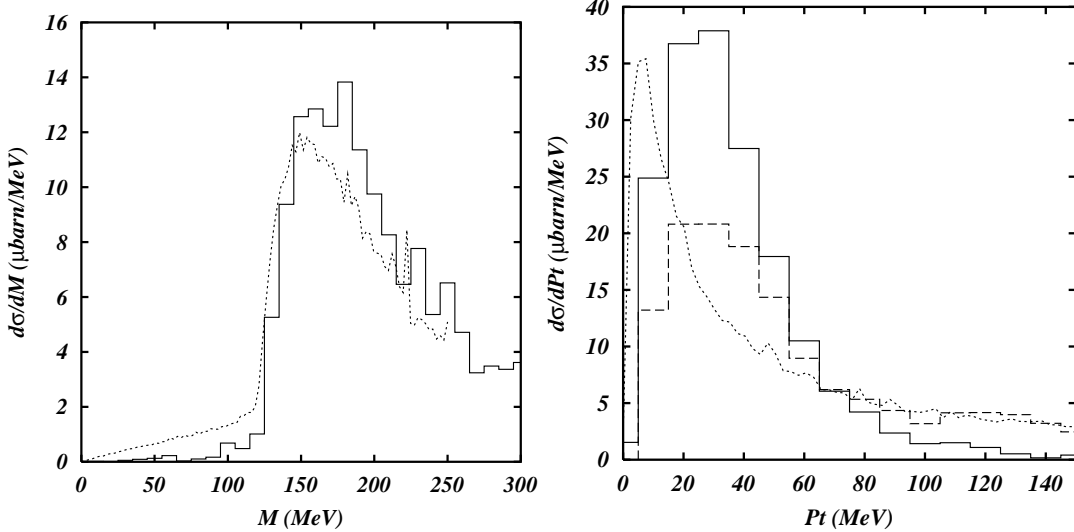


Figure 5: The invariant mass and the transverse momentum of the e^+e^- pair are shown. Again the results are compared with the unrestricted cross section (dotted line). In addition we have plotted the result of the restricted calculation without form factor (dashed line). Both results have been normalized to give the same total cross section.

total cross section

$$\sigma_{total} = \sum_{N=1}^{\infty} \sigma(N) \quad (17)$$

The cross section one would get from the Born cross section can be interpreted as a “multiplicity” cross section

$$\sigma_{Born} = \int d^2b P^2(GDR, b) P(b) = \sum_{N=1}^{\infty} \sigma(N) \quad (18)$$

and would be relevant in order to calculate the number of pairs produced (in contrast to the number of events). One can see that about 10% of all events are multiple pair production events and accordingly also about 10% of all pairs are produced in a multiple pair production process. This shows that at ALICE one should be able to detect and study multiple pair production.

We have investigated a similar question also for RHIC using as an estimate for a possible range $p_t > 50$ MeV/c and $2.5 < y < 4.0$. Unfortunately the probability for pair production under these conditions is only of the order of a few permille and therefore the multiple pair production cross section is less than one permille of the single pair production cross section, making such an investigation difficult.

4 Discussion and Outlook

We have calculated total and differential cross section of the pair production process in ultraperipheral heavy ion collisions in lowest order QED for the simultaneous electromagnetic excitation of both ions. We have seen that the most sensitive quantity is the transverse momentum distribution, which differs mostly from the distribution of the

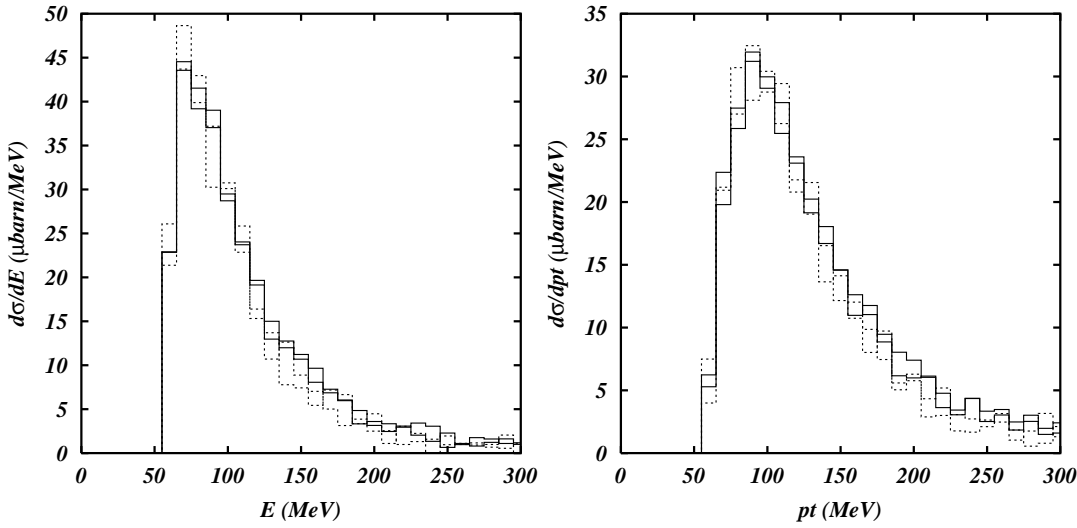


Figure 6: Energy and transverse momentum distribution are shown for the two leptons for PbPb collisions at the LHC (solid line). This is compared with the rescaled spectrum of AuAu collisions at RHIC (dotted line).

unrestricted cross section. As the comparison will show [19, 2] our results were found to be in good agreement with the experimental results. On the other hand only about 50 events were found at STAR, so the overall statistics is not very good. Additional runs might give better statistics. Still our analysis shows that the data at the moment give no sign that higher order Coulomb effects are large for pairs produced with these large transverse momenta [31]. Such higher order Coulomb effects would lead most likely to an asymmetry of the electron and positron distribution especially for the transverse momentum distribution. At the moment however no calculation exists, which describes consistently the effects of the strong Coulomb fields of both pairs on the pair production process at small impact parameter. The experimental condition of RHIC does not allow to look for multiple pair production effects as the probability for pair production with these conditions is well below one.

As already mentioned above the transverse momentum cut of $p_t > 65$ MeV/c at STAR was only possible due to a reduced magnetic field. There are currently plans to use even lower magnetic fields and also making use of other detectors within STAR [32] in order to extend the measurements both to smaller transverse momenta and to larger rapidities. It remains to be seen, whether the new phenomenon of multiple pair production, will then be detected. On the other hand with the low transverse momentum cutoff of the ITS at ALICE/LHC, about 10% of all pair production events are going to be multiple pair production processes, therefore one should expect that this new phenomena will be observed easily there. The fact that no kinematical information and also no particle identification is possible at ALICE, will make such a measurement still a challenge.

5 Acknowledgement

The authors would like to thank Spencer R. Klein and Vladimir B. Morozov for interesting discussions and collaborations on this subject and (S. K.) for critical reading of the

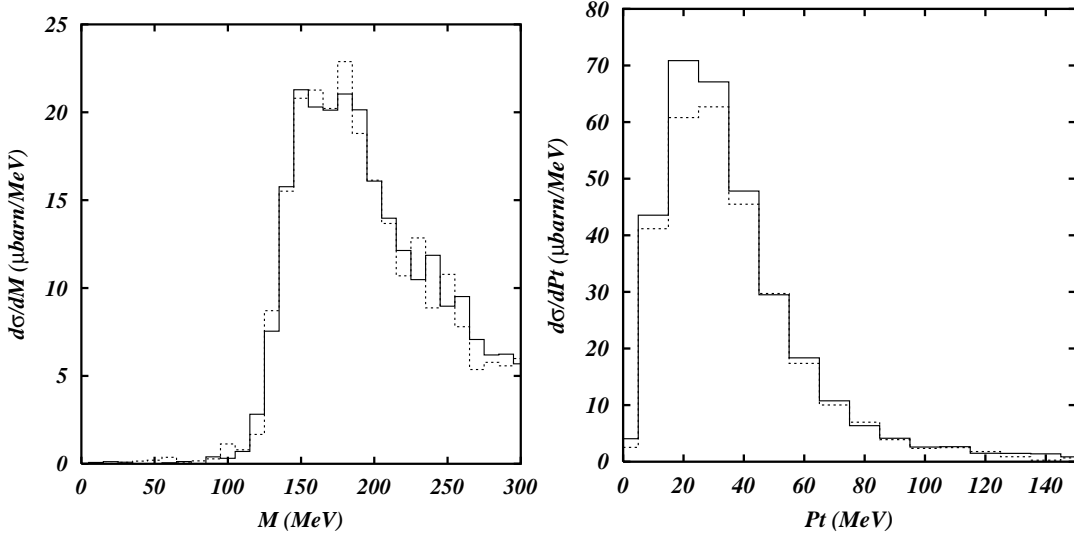


Figure 7: The invariant mass and the transverse momentum of the e^+e^- pair is shown for PbPb collisions at the LHC (solid line). The results are compared with the rescaled spectrum of AuAu collisions at RHIC (dotted line).

manuscript. Discussions with Serguei Sadovsky and Yuri Kharlov have been important in understanding the possibilities of detecting the pair production at LHC.

6 Appendix

Throughout our calculations we have assumed that only the GDR excitation is relevant for the triggering and therefore a simplified dependence on b , see Eq. (4) has been used. In this appendix we want to show that this is not a real limitation, but that other impact parameter dependencies can be treated as well. For example assuming that the higher resonant states of the GDR are excited through a Poisson process, we would need to replace $P_{GDR}(b)$ by $1 - \exp(-P_{GDR}(b))$. In general we assume that the relevant $P_{A \rightarrow A^* \rightarrow X+xn}(b)$ can be expressed as a series of inverse powers of b

$$P_{A \rightarrow A^* \rightarrow X+xn}(b) = \sum_{n=0}^{\infty} \frac{S_n}{b^n} \quad (19)$$

Using this in the expression for $d^6\sigma_{e^+e^-, 2GDR}/(d^3p_+d^3p_-)$, see Eq. (14), we need to calculate generalizations of $I(z)$, Eq. (11) of the form

$$I_n(z) := \int_z^{\infty} \frac{dx}{x^n} J_0(x) \quad (20)$$

with $I_3(z)$ corresponding to the one used in our calculations.

For the calculation of these integrals, we first use the following recursion relation

$$I_n(z) = \frac{J_0(z)}{(n-1)z^{n-1}} - \frac{J_1(z)}{(n-1)^2 z^{n-2}} - \frac{1}{(n-1)^2} I_{n-2}(z) \quad (21)$$

This relation can be easily derived by partial integration and by using the well-known recursion relations between the Bessel functions $J_n(z)$ [33]. By repeated application of

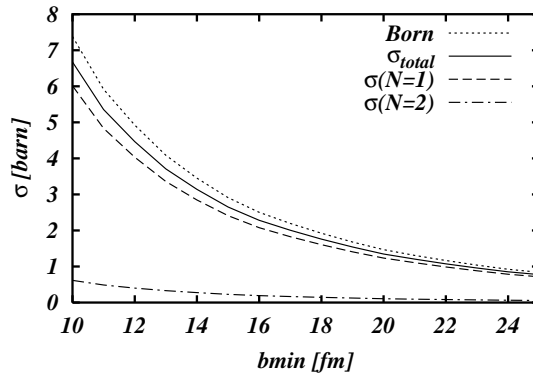


Figure 8: The different cross sections for single and multiple pair production are shown for the kinematical conditions at ALICE. The cross section is shown as a function of b_{min} , the minimal impact parameter. See the text for further details of the different cross sections.

Eq. (21) every I_n with odd and even n can be reduced to the starting values $I_1(z)$ and $I_0(z)$, respectively, which are given in the literature [33]:

$$I_0(z) = 1 - z {}_1F_2\left(\frac{1}{2}; 1, \frac{3}{2}; -\frac{z^2}{4}\right) \quad (22)$$

and

$$I_1(z) = \frac{z^2}{8} {}_2F_3\left(1, 1; 2, 2, 2; -\frac{z^2}{4}\right) - \ln \frac{z}{2} - \gamma \quad (23)$$

where γ is the Euler constant.

These two expressions can be calculated easily by the rapidly converging power series of the hypergeometric functions or by using suited polynomial expressions given in the literature [33]. We are here only interested in the case, where $n = 2m + 1$ is an odd number, in which case the complete recursion relation is given by

$$I_{2m+1}(z) = \frac{(-1)^m}{m!^2 2^{2m+1}} \left\{ J_0(z) \sum_{s=1}^m s!(s-1)! \left(-\frac{4}{z^2}\right)^s - \frac{z}{2} J_1(z) \sum_{s=1}^m (s-1)!^2 \left(-\frac{4}{z^2}\right)^s + I_1(z) \right\}. \quad (24)$$

Moreover this equation can be further simplified, by splitting off the terms singular at $z = 0$ (the principal part of the Laurent expansion in z), by using the power series for the Bessel functions:

$$J_m(z) = \left(\frac{z}{2}\right)^m \sum_{k=0}^{\infty} \frac{(-z^2/4)^k}{k!(k+m)!} \quad (25)$$

and by rearranging the resulting sum. After some straightforward algebra we thus obtain the compact expression for $m \geq 0$

$$I_{2m+1}(z) = \frac{(-1)^m}{2^{2m+3}(m+1)!^2} z^2 {}_2F_3\left(1, 1; 2, 2+m, 2+m; -\frac{z^2}{4}\right) \quad (26)$$

$$- \frac{(-1)^m}{2^{2m}(m)!^2} \left(\ln \frac{z}{2} + \gamma\right) + \sum_{k=0}^m a_{m,k} z^{-2k} \quad (27)$$

where

$$a_{m,0} = \frac{(-1)^m}{2^{2m}m!^2} \sum_{s=1}^m \frac{1}{s}, \quad a_{m,k} = \frac{(-1)^{m-k}}{2^{2(m-k)+1}(m-k)!^2 k} \quad k \geq 1 \quad (28)$$

For $m = 1$ we get the explicit expression

$$I_3(z) = \frac{1}{2z^2} + \frac{1}{4} \left(\ln \frac{z}{2} + \gamma - 1 \right) - \frac{1}{128} z^2 {}_2F_3(1, 1; 2, 3, 3; -z^2/4) \quad (29)$$

and similarly for $m = 2$. Again the hypergeometric function in Eq. (27) can well be calculated numerically by its power series:

$${}_2F_3 \left(1, 1; 2, 2 + m, 2 + m; -\frac{z^2}{4} \right) = (m+1)!^2 \left(-\frac{4}{z^2} \right) \sum_{k=1}^{\infty} \frac{\left(-\frac{z^2}{4} \right)^k}{k(k+m)!^2}. \quad (30)$$

We use this rapidly converging power series in our numerical calculations. For the case where n is an even number, the same approach can be used. For completeness we only give here the final result:

$$I_{2m}(z) = \frac{1}{2^{2m-1}(2m-1)} {}_1F_2 \left(-m + \frac{1}{2}; -m + \frac{3}{2}, 1; -\frac{z^2}{4} \right) + \frac{(-1)^m 2^{2m} m!^2}{(2m)!^2}. \quad (31)$$

References

- [1] K. Hencken, D. Trautmann, and G. Baur, Phys. Rev. A **51**, 1874 (1995).
- [2] F. Meissner and V. B. Morozov, Coherent electromagnetic processes in ultra-peripheral heavy-ion collisions, nucl-ex/0307006, 2003.
- [3] V. B. Morozov, Ph.D. thesis, University of California, Berkeley, 2003, LBNL-53583.
- [4] S. Klein, Ultra-peripheral collisions with STAR at RHIC, nucl-ex/0310020, 2003.
- [5] A. J. Baltz, S. R. Klein, and J. Nystrand, Phys. Rev. Lett. **89**, 012301 (2002).
- [6] S. Klein and J. Nystrand, Phys. Rev. Lett. **84**, 2330 (2000).
- [7] S. Klein and J. Nystrand, Phys. Rev. C **60**, 014903 (1999).
- [8] A. Baltz, C. Chasman, and S. N. White, Nucl. Instrum. Methods **417**, 1 (1998).
- [9] M. Chiu *et al.*, Phys. Rev. Lett. **89**, 012302 (2002).
- [10] G. Baur *et al.*, Nucl. Phys. **A729**, 787 (2003).
- [11] G. Baur, in *CBPF Int. Workshop on relativistic aspects of nuclear physics, Rio de Janeiro, Brazil 1989*, edited by T. Kodama *et al.* (World Scientific, Singapore, 1990), p. 127.
- [12] G. Baur and L. G. Ferreira Filho, Nucl. Phys. A **518**, 786 (1990).
- [13] M. Greiner, M. Vidović, J. Rau, and G. Soff, J. Phys. G **17**, L45 (1991).

- [14] N. Cahn and J. D. Jackson, Phys. Rev. D **42**, 3690 (1990).
- [15] G. Baur, K. Hencken, and D. Trautmann, Topical Review, J. Phys. G **24**, 1657 (1998).
- [16] V. M. Budnev, I. F. Ginzburg, G. V. Meledin, and V. G. Serbo, Phys. Rep. **15**, 181 (1975).
- [17] M. Vidović, M. Greiner, C. Best, and G. Soff, Phys. Rev. C **47**, 2308 (1993).
- [18] G. Baur and N. Baron, Nucl. Phys. A **561**, 628 (1993).
- [19] S. Klein and STAR collaboration, Observation of e^+e^- leptons in UPC, in preparation, 2004.
- [20] C. A. Bertulani and G. Baur, Phys. Rep. **163**, 299 (1988).
- [21] A. J. Baltz, M. J. Rhoades-Brown, and J. Weneser, Phys. Rev. E **54**, 4233 (1996).
- [22] A. J. Baltz and M. Strikman, Phys. Rev. D **57**, 548 (1998).
- [23] I. A. Pshenichnov *et al.*, Phys. Rev. C**64**, 024903 (2001).
- [24] I. A. Pshenichnov *et al.*, Phys. Rev. C**60**, 044901 (1999).
- [25] I. A. Pshenichnov *et al.*, Phys. Rev. C **57**, 1920 (1998).
- [26] A. Alischer, K. Hencken, D. Trautmann, and G. Baur, Phys. Rev. A **55**, 396 (1997).
- [27] G. P. Lepage, J. Comput. Phys. **27**, 192 (1978).
- [28] K. Hencken, D. Trautmann, and G. Baur, Phys. Rev. A **51**, 998 (1995).
- [29] M. C. Güçlü *et al.*, Phys. Rev. A **51**, 1836 (1995).
- [30] G. Baur *et al.*, Phys. Rep. **364**, 359 (2002).
- [31] S. J. Brodsky and J. Gillespie, Phys. Rev. **173**, 1011 (1968).
- [32] S. Klein, private communication.
- [33] M. Abramowitz and I. A. Stegun, *Handbook of mathematical Functions* (Dover, New York, 1965).